Lifetimes of C_{60}^{2-} and C_{70}^{2-} dianions in a storage ring

S. Tomita[a] and J. U. Andersen[b]
Department of Physics and Astronomy, University of Aarhus, Aarhus C DK-8000, Denmark

H. Cederquist
Department of Physics, Stockholm University, SCFAB, Stockholm SE-106 91, Sweden

B. Concina
Department of Physics and Astronomy, University of Aarhus, Aarhus C DK-8000, Denmark

O. Echt
Department of Physics, University of New Hampshire, Durham, New Hampshire 03824

J. S. Forster
Département de Physique, Université de Montreal, Quebec H3C 3J7, Canada

K. Hansen
Department of Physics, Göteborg University, Gothenburg SE-41296, Sweden

B. A. Huber
Centre Interdisciplinaire de Recherche Ions Lasers, rue Claude Bloch, B.P. 5133, 14070 Caen Cedex 5, France

P. Hvelplund
Department of Physics and Astronomy, University of Aarhus, Aarhus C DK-8000, Denmark

J. Jensen
Department of Physics, Stockholm University, SCFAB, Stockholm SE-106 91, Sweden

B. Liu
Department of Physics and Astronomy, University of Aarhus, Aarhus C DK-8000, Denmark

B. Manil and L. Maunoury
Centre Interdisciplinaire de Recherche Ions Lasers, rue Claude Bloch, B.P. 5133, 14070 Caen Cedex 5, France

S. Brøndsted Nielsen
Department of Physics and Astronomy, University of Aarhus, Aarhus C DK-8000, Denmark

J. Rangama
Centre Interdisciplinaire de Recherche Ions Lasers, rue Claude Bloch, B.P. 5133, 14070 Caen Cedex 5, France

H. T. Schmidt and H. Zettergren
Department of Physics, Stockholm University, SCFAB, Stockholm SE-106 91, Sweden

(Received 12 September 2005; accepted 22 November 2005; published online 10 January 2006)

C_{60}^{2-} and C_{70}^{2-} dianions have been produced by electrospray of the monoanions and subsequent electron pickup in a Na vapor cell. The dianions were stored in an electrostatic ring and their decay by electron emission was measured up to 1 s after injection. While C_{70}^{2-} ions are stable on this time scale, except for a small fraction of the ions which have been excited by gas collisions, most of the C_{60}^{2-} ions decay on a millisecond time scale, with a lifetime depending strongly on their internal temperature. The results can be modeled as decay by electron tunneling through a Coulomb barrier, mainly from thermally populated triplet states about 120 meV above a singlet ground state. At times longer than about 100 ms, the absorption of blackbody radiation plays an important role for the decay of initially cold ions. The tunneling rates obtained from the modeling, combined with WKB estimates of the barrier penetration, give a ground-state energy 200±30 meV above the energy of the monoanion plus a free electron and a ground-state lifetime of the order of 20 s.
 [DOI: 10.1063/1.2155435]

[a]Present address: Institute of Applied Physics, University of Tsukuba, Tsukuba, Ibaraki 305-0006, Japan.
[b]Electronic mail: jua@phys.au.dk

I. INTRODUCTION

In recent years there has been a great interest in free, doubly charged anions.[1,2] Owing to the electron-electron Coulomb repulsion, atomic dianions are not stable and the binding of two electrons in a molecule depends strongly on its size.[3] The second electron is confined by a Coulomb barrier, and even for negative binding energy the lifetime for tunneling through this barrier can be very long. The fullerenes are ideal for studying the dependence of the stability of dianions on the size of the molecule, and C_{2n}^{2-} with $2n \geqslant 70$ have been produced directly in the gas phase by electrospray.[4,5] These dianions can also be formed by electron attachment to monoanions in a Penning trap.[6,7]

The most interesting case, the dianion of buckminsterfullerene C_{60}^{2-}, has been something of a puzzle. The lowest unoccupied electronic level of C_{60} is sixfold degenerate, including spin. It can be populated by the reduction of C_{60} in solution, and the resulting ions have been investigated by many techniques, e.g., by electron-spin resonance (ESR) and optical spectroscopy.[8] However, the spectra are difficult to interpret, and the contributions from different charge states are difficult to disentangle unambiguously. The free dianion of C_{60} is predicted to be at the limit of stability with a small negative affinity for the second electron.[9–11] This ion has been identified by mass spectrometry in an ion trap after laser desorption of fullerenes from a surface,[12,13] and from observation of the survival time of the signal a lifetime of more than 3 min was inferred.[12] However, it has not been possible to create the dianion in a more controlled manner, e.g., by electrospray or by attachment of a free electron to the monoanion.

The lowest unoccupied orbitals in C_{60} have t_{1u} symmetry, and the coupling of two electrons is analogous to the *LS* coupling of two *p* electrons in an atom and results in ^1A_g, ^3T_g, and ^1H_g multiplets analogous to the ^1S, ^3P, and ^1D atomic terms. It turns out that the theory of atomic multiplets can be applied to calculate the term splittings and, in accordance with Hund's rules, the energy from Coulomb repulsion between the two electrons is lowest in the triplet states and highest in the ^1A_g state.[14] The Coulomb energy can be lowered by mixing with orbitals in the neighboring t_{1g} level; the wave functions have opposite parity, and hence "hybridized" wave functions may be created by linear combination, which are localized far apart in the molecule.[15] The effect of mixing depends strongly on the energy splitting between the t_{1u} and t_{1g} levels; for the measured optical transition energy of $\sim$1.3 eV, the triplet level remains lowest, but the splitting of the three dianion levels is considerably reduced according to a recent calculation.[16]

The electrons are also stabilized by Jahn-Teller distortions of the molecule and this may change the order of the levels. The description of the Jahn-Teller effect in C_{60} ions has been the subject of much theoretical work.[14,17–21] From an analysis of a measured spectrum of photoelectrons from C_{60}^- it was concluded that the coupling is stronger by a factor of 2–3 than that predicted at the time by theory.[22] This is supported by more recent theoretical calculations which reproduce the photoemission spectrum quite well.[23] The Jahn-Teller effect should be even stronger for singlet dianions in which the two additional electrons can occupy the same orbital.[14]

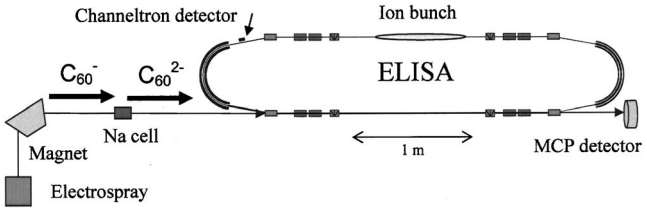

FIG. 1. Sketch of the electrostatic ring ELISA.

The interest in the anions of C_{60} has been spurred by the discovery of superconductivity in C_{60}^- based materials at quite high temperatures. It is generally accepted that the electron pairing leading to superconductivity must be local, and some authors suggest that it originates in a strong intramolecular coupling to vibrations.[17,22,24–26] Others emphasize the correlation of electronic origin, such as the configuration interaction with the neighboring single-electron level mentioned above,[27,28] and some even claim that Jahn-Teller distortions cannot possibly contribute to superconductivity.[29] Both term splittings due to exchange interaction and Jahn-Teller stabilization were considered in a recent discussion, but the effect of mixing with the t_{1g} orbitals was not included explicitly.[30,31]

A useful starting point is to try to understand the properties of the isolated C_{60} anions. Even for the monoanion, there is uncertainty in the interpretation of the optical spectra and their dependence on the solvent.[8] The most recent interpretation of ESR measurements on dianions in solution is a singlet ground state with a close-lying triplet state, which can be thermally populated.[8,32] However, since the separation between the levels is only a tenth of an eV, the interaction with the surrounding matrix could affect the ordering. There is a need for experiments on isolated C_{60} anions to provide results which can serve as benchmarks for theory. We have recently measured the near-infrared-absorption spectrum for C_{60}^- in the gas phase and have proposed an identification of the observed bands.[33] The electronic states of the doubly charged anion are of particular interest in that they reveal the magnitude of the effective gas-phase Coulomb and exchange interactions.[9] We have succeeded in creating beams of C_{60}^{2-} with sufficient intensity to allow a study of the lifetime in a storage ring.[34] For comparison, we have also observed C_{70}^{2-} which has been reported to have a lifetime of 80 s in an ion trap at room temperature.[5]

II. EXPERIMENTAL DETAILS

The experiments were carried out at the small electrostatic ion storage ring, Aarhus (ELISA),[35] which is illustrated in Fig. 1. The injection of ions from solution with an electrospray ion source is described in detail in Refs. 36 and 37. Singly charged anions of C_{60} (or C_{70}) were sprayed from a solution of C_{60} (or C_{70}) and tetrathiafulvalene in toluene and dichloromethane. They were stored for typically 0.1 s in a linear ion trap with a He trapping gas at a temperature between 225 and 355 K. The temperature of the trapping gas

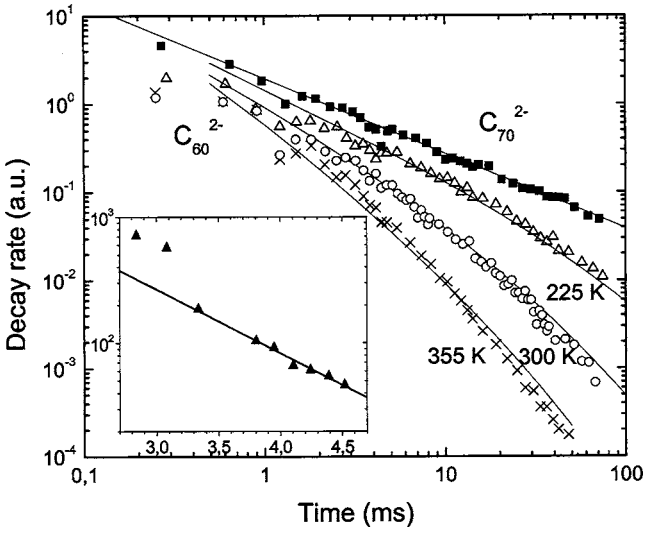

FIG. 2. Electron emission in the storage ring, detected as a signal from C_{70}^- or C_{60}^- in a channeltron placed after a 10° electrostatic deflector. The injected ions were C_{70}^{2-} (■) and C_{60}^{2-} from charge exchange of monoanions with initial temperatures of 225 K (△), 300 K (o), and 355 K (x). Each point corresponds to the sum of counts for several revolutions of the ion bunch. The different data sets are not normalized relative to each other. The curves through the points are a power law with $n=-0.85$ for C_{70}^{2-} and from the simulations described in the text for C_{60}^{2-}. The insert shows an Arrhenius plot of the cutoff rate $1/\tau$ (s^{-1}) versus $1000/T_{trap}$ (K^{-1}).

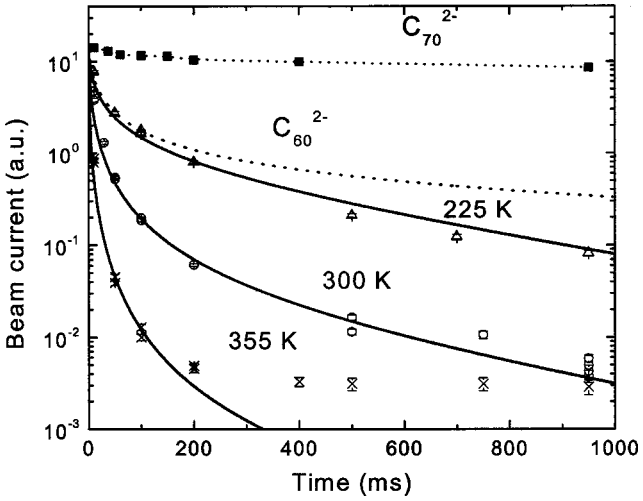

FIG. 3. Time dependence of the number of ions stored in the ring, measured by dumping the beam onto a microchannel detector with a varying delay after the injection. The injected ions were C_{70}^{2-} (■) and C_{60}^{2-} from charge exchange of monoanions from a trap with temperatures of 225 K (△), 300 K (o), and 355 K (x). The full curves are from simulations with the model described in the text. The dashed curve for 225 K is obtained from simulations without the emission and absorption of photons.

was calibrated with measurements of the lifetime for UV-photon-induced fragmentation of a tripeptide Lys-Trp-Lys-H^+ for which the Arrhenius decay parameters had been determined from the variation of the lifetime with laser wavelength.[38]

After ejection from the trap, acceleration to 22 keV, and mass selection with a magnet, ion bunches were passed through a cell containing Na vapor. As demonstrated in Ref. 34, about 30% of the ions may be converted to doubly charged anions by electron capture in collisions with Na atoms. The electrical fields in the storage ring were first adjusted to store singly charged ions and then reduced by a factor of 2 to select the doubly charged ions. The pressure in the ring was a few times 10^{-11} mbar, and for stable fullerence anions the storage lifetime was limited by collisions with the residual gas to ~10 s.

The decay of metastable ions by electron emission was recorded by the detection of monoanions with a channeltron placed close to the stored beam after a 10° deflection inside the ring (Fig. 1). There were periodic variations in the yield associated with betatron oscillations of the beam position in the ring, the most pronounced period corresponding to about three revolutions, but these oscillations were strongly damped by the averaging of counts from several revolutions. The revolution time was 108.15 μs for C_{60} ions. The measurements were repeated with a 10 Hz injection rate and with a dump of the beam at the end of each observation period of 80 ms. For observations on a longer-time scale, up to 1 s, a corresponding lower injection rate was selected.

The decay of the stored beams was also measured directly. At varying times after injection, the beam was dumped onto a microchannel plate, positioned at the end of the injection side of the ring (Fig. 1). The decay of a short-lived beam can in this way be followed over several orders of magnitude. A normalization to the injected beam current is required, and for dumps later than 10 ms after injection the signal was normalized to the sum of the channeltron counts over the first 10 ms. However, it is difficult to normalize beam dumps after much shorter storage times.

III. RESULTS

Results obtained with the two methods of observation are shown in Figs. 2 and 3. The curves in these figures are from modeling, and they will be discussed later. For the qualitative interpretation, it is useful first to consider the direct measurements of beam decay in Fig. 3. For C_{70}^{2-}, only a relatively small decrease in the beginning is observed. Our interpretation is that the dianion is stable at room temperature on a time scale of seconds. The small initial reduction of the beam is due to the decay of ions that have been excited in collision with residual gas atoms, mainly just after exit from the trap.[39] Since the binding energy of the second electron is very low, an excitation of a few eV should be sufficient to induce decay on a millisecond time scale. The depletion is much stronger for the C_{60}^{2-} beams, and it depends on the temperature of the trap. This implies that at the trap temperatures these dianions are not stable on a time scale of seconds.

The time dependence of the counts in the channeltron, shown in Fig. 2, gives more detailed information about the decay. The power law with power close to −1 observed for C_{70}^{2-} is characteristic for an ensemble of isolated molecules with a broad distribution in excitation energy.[39,40] The energy distribution is gradually depleted from the high-energy side, and at time t ions with rate constant $k(E) \sim 1/t$ dominate the yield. The results for C_{60}^{2-} are quite different. At the shortest times, the variation of the decay rate is similar to that observed for C_{70}^{2-} but the rate decreases much more steeply after a characteristic time τ which depends on the tempera-

ture T_{trap} of the ions in the trap, before electron capture. There is a lower cutoff of the internal energy distribution at the thermal energy corresponding to T_{trap} and the power-law dependence of the decay rate is changed into a nearly exponential decrease when at time τ the depletion of the distribution reaches this energy.

Since at this time the power-law decay is dominated by ions with rate constant $\sim 1/\tau$, we can interpret τ as the lifetime of ions with temperature T_{trap}. The data can be represented quite well by a function proportional to $t^{-0.6}\exp(-t/\tau)$, and we have derived the dependence of τ on trap temperature from fits with this function. The results are shown in an Arrhenius plot in the insert in Fig. 2. Below room temperature, the points fall on a line corresponding to an activation energy of ~0.1 eV. Above room temperature, there are clear deviations from this line although the determination of the cutoff is more uncertain for small τ. A more detailed interpretation is derived from the modeling discussed in the following but it is noteworthy that one of our main results, the decay of C_{60}^{2-} by a thermally activated process, can be derived with few assumptions directly from the data.

We now return to Fig. 3 where the C_{60}^{2-} decay is followed to longer times. The time dependence is straightforward to interpret qualitatively for the two lower trap temperatures: the decay is dominated by a thermally activated process, presumably electron emission via tunneling from an excited state about 0.1 eV above the ground state. The distribution of microcanonical temperatures in the ensemble of stored ions has a lower cutoff around the trap temperature but this cutoff is not sharp, so the distribution has a tail towards lower temperatures. At low temperature, mainly the ground state is populated, and if the ground-state lifetime is long there should be a small fraction of quite stable molecules, as is indeed observed. It turns out that the distributions can be reproduced quantitatively by modeling if the absorption of blackbody radiation is taken into account.

The only puzzling feature in Fig. 3 is the observation of a small, very long-lived component for the highest trap temperature. That something abnormal is happening in the measurement for this temperature is illustrated in Fig. 4, showing the intensity of the dumped beam at 10 and 500 ms for a series of temperatures. At both dump times, the variation is smooth, very close to exponential, except for the measurement at 500 ms for 355 K which is clearly abnormal.

IV. BEAM IMPURITY

The observation of a small stable component of the C_{60}^{2-} beam at the highest temperature (355 K), as shown in Fig. 3, was a surprise, and in view of the very low level of this signal, it was important to consider possible artifacts. One possibility is a small component of the beam with very low internal excitation energy. The ions are cooled by the adiabatic expansion in the spray source, and one might imagine that a small fraction does not come into thermal equilibrium with the He gas in the ion trap. However, we varied the storage time in the ion trap without any change in the results.

Electronic noise related to the rapid switching of high-voltage power supplies has been a problem for the beam dumps after long storage times, with very low counting rates. However, there is a large variation in the ratio between the number of such switches and the channeltron counts, and the proportionality for the highest temperature of the number of dumped ions to the counts in the channeltron (Fig. 3) proves that, even in this case, the dump signal is mainly beam related and not electronic noise.

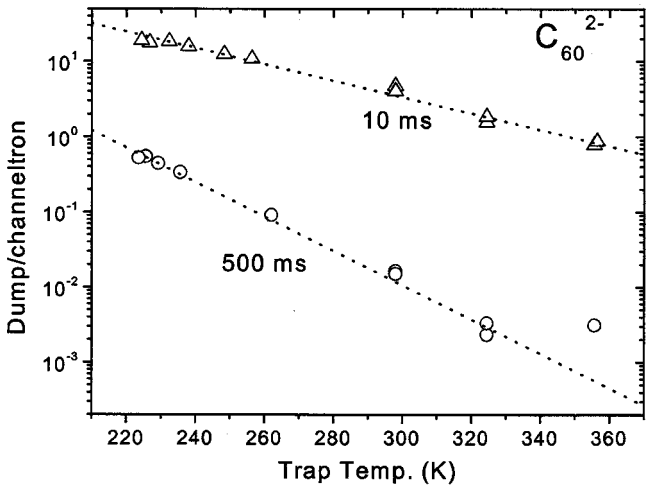

FIG. 4. C_{60}^{2-} beam current at 10 and 500 ms, normalized to the counts in the channeltron during the first 10 ms. Measurements for different ion trap temperatures.

Another possible explanation is an impurity with the same mass and charge as C_{60}^{-} that also picks up an electron in the Na cell. Indeed, there are weak beams transmitted through the magnet at mass numbers just below 720. We have tested this possibility by measuring the isotope distribution of the beam. With a natural abundance of 1.108% for ^{13}C, the expected ratios of masses 720, 721, and 722 for C_{60} are 100:67:22. The mass ratios in the observed beam depend on the magnetic field of the analyzer but should be independent of storage time if there are no contaminants. As illustrated in Fig. 5, we could measure the isotopic time splitting

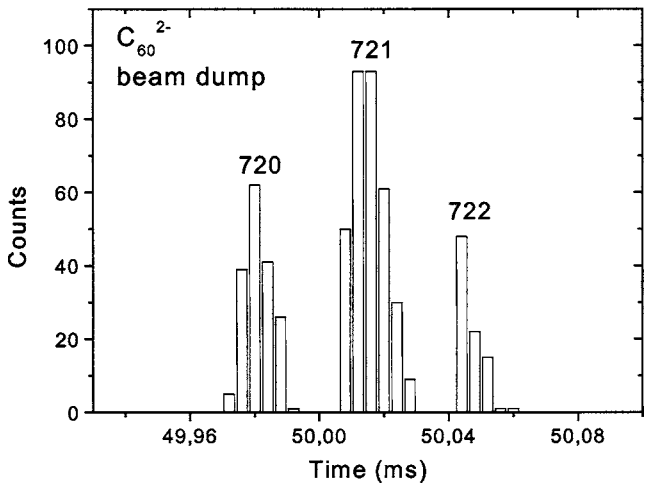

FIG. 5. Time spectrum of the counts in the microchannel-plate detector for beam dump at 50 ms after injection into the ring of C_{60}^{2-} ions. The expected time difference between molecules with mass 720 and 721 is 35 μs. The magnet was optimized for transmission of mass 721.

of the dumped beam. Since ions with different masses have the same energy, their velocity is inversely proportional to the square root of their mass, and the time difference between the arrival of neighboring isotopes 720 and 721 at dump time t is $t/1440$. The splitting should therefore be 35 μs for $t=50$ ms, in good accord with the measurement. Although we have not been able to obtain conclusive evidence for the isotopic composition at the later times because the statistics and resolution are poor, indications are that it is unchanged.

Unfortunately, a test of the isotopic composition does not provide a very strong discrimination against impurities. The most likely "impurities" are the isomers of C_{60} without the closed cage structure. When fullerenes are produced by the laser ablation of graphite, only a small fraction of the molecules with mass 720 are fullerenes,[41] and it is possible that there could be a small fraction of configurational isomers in the fullerene powder we have used. It is plausible that dianions of such isomers could be formed efficiently in the Na cell and that they could be stable because the Coulomb repulsion is smaller in more extended molecules.

We conclude that the most likely explanation for the small long-lived component at 355 K is an impurity, maybe a configurational isomer. Figure 4 shows that the inpurity signal is probably not significant for the measurements at lower temperatures in Fig. 3.

V. ENERGY LEVELS FROM NEAR-INFRARED SPECTROSCOPY

With the storage of a C_{60}^{2-} beam in ELISA the possibility of laser spectroscopy on the dianion has opened up, and this provides more information on the energy levels, in particular, on the question whether the ground state is triplet or singlet. We have measured the near-infrared-absorption spectrum in the storage ring by the detection of monoanions produced by electron detachment after the absorption of a photon from a laser pulse. The absorption spectra are quite similar to spectra for dianions in solution,[42,43] with the main absorption band near 945 nm. There is a strong signal in the channeltron from emission within the first ~10 μs after the absorption and also a much weaker signal from delayed emission after a few revolutions in the ring. Thus, in the excited state ~1.3 eV above the ground state, with one electron in a t_{1g} electronic orbital, the electron can be confined by the Coulomb barrier long enough for the conversion of the electronic excitation to vibrations. The measurements will be discussed in detail elsewhere,[44] and only the results of direct relevance to the modeling of the decay will be mentioned here.

The similarity to the absorption spectra in solution indicates that the ground state is singlet[32] also in the gas phase. The symmetry of the ground state should then be A_g and there should be a low-lying excited state with H_g symmetry and a degeneracy of 5.[14] Formally, the population of these states corresponds to the combination of two $l=1$ electrons to angular momenta $L=0$ and $L=2$, although the nature of strongly coupled Jahn-Teller states is quite different.[14] Consistent with these predictions, the spectroscopy has revealed the presence of a ground state which is populated strongly only at very low temperatures, and the splitting between the two singlet states ^1A_g and ^1H_g is determined to be 22 meV.[44]

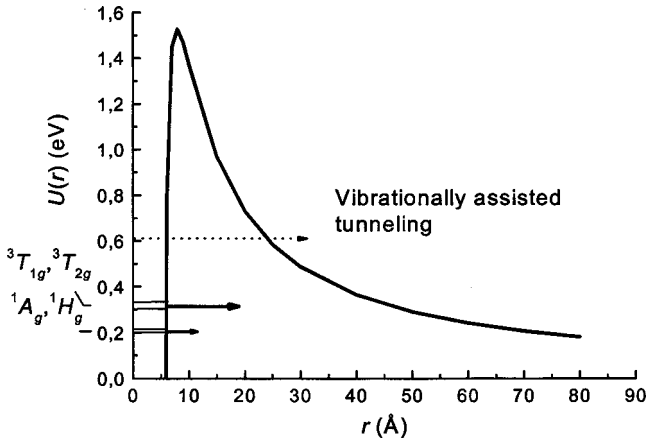

FIG. 6. Potential barrier for $l=1$ [Eq. (1)]. The levels indicated originate in the coupling of two t_{1u} electronic orbitals into singlet and triplet states. Channels for tunneling are indicated by arrows.

For the triplet state, the Jahn-Teller problem is identical to that for the monoanion.[14] The symmetries of the lowest two levels should be $^3T_{1g}$ and $^3T_{2g}$, and from gas-phase spectroscopy on C_{60}^- the splitting has been determined to be 30 meV.[33] Both levels have triple orbital degeneracy in addition to the spin degeneracy.

VI. COULOMB BARRIER

The second electron in the dianion is confined by a Coulomb barrier, and the lifetime of states with positive energy is determined mainly by the probability for tunneling through the barrier. The effective potential has three components, the electrostatic repulsion from a charge $-e$ at the center, an attraction due to the polarization of the anion, and a repulsive angular momentum barrier corresponding to $l=1$.[11] We treat the anion as a conducting sphere with radius $R=4.5$ Å, corresponding to a polarizability ~15% larger than that for neutral C_{60}.[45] The polarization potential may then be obtained from a standard calculation of image charges, and we obtain the effective potential,

$$V(r)=\frac{e^2}{r}-\frac{e^2R^3}{2r^2(r^2-R^2)}+\frac{e^2a_0}{r^2}, \tag{1}$$

where $a_0=0.53$ Å is the Bohr radius. This potential is illustrated in Fig. 6. The excited electronic level with one electron in a t_{1g} orbital is very close to the maximum of the potential, and the observation in Ref. 44 of internal conversion after photoexcitation to this level is therefore strong evidence against a considerably lower barrier for electron emission, as suggested by the analysis of photoemission measurements for heavier fullerenes in Ref. 46.

An electron with positive energy E can tunnel through the barrier with a rate given in the WKB approximation by

$$k=\nu\exp(-W), \quad W=\frac{2}{\hbar}\int_{r_1}^{r_2}\sqrt{2m(V(r)-E)}dr, \tag{2}$$

where the limits of the integral are the classical turning points. A rough estimate of the attempt frequency ν can be

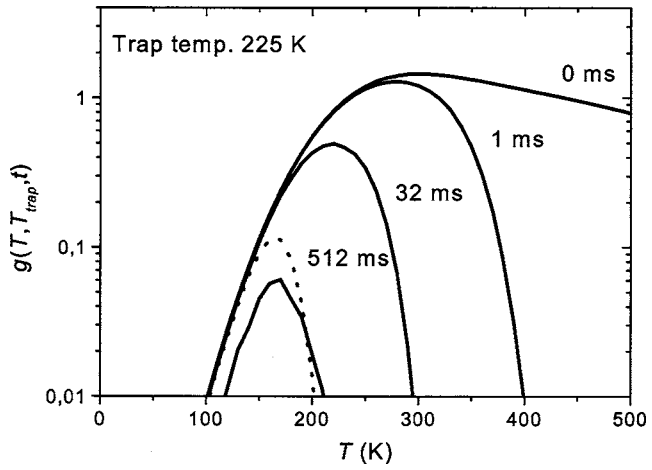

FIG. 7. Distribution of the C_{60}^{2-} ion ensemble over internal temperatures (microcanonical) at different times. Dashed curve without the emission and absorption of photons.

obtained from the uncertainty principle, $\nu \approx \hbar/mR^2 \cong 6 \times 10^{14}$ s^{-1}. However, this value should probably be reduced considerably due to a poor match of an emitted p wave to a bound state with strong $l=5$ character.[10,11] Below we use a frequency factor which is lower by a factor of 20, and we estimate the uncertainties associated with a further reduction.

VII. MODELING OF THE DECAY RATES

The simplest interpretation of the temperature-dependent decay rate is tunneling from thermally populated excited states. We have modeled the observations with an internal energy distribution $g(\varepsilon, T_{\text{trap}})$ that is a convolution of the initial thermal distribution of the internal energy of the monoanions at temperature T_{trap} with an exponential distribution of the excitation energy. Mathematically, this is a very simple one-parameter distribution, and as we shall see (Fig. 7), the experiment only probes a very narrow range of energies and hence is insensitive to the detailed shape of this distribution. The excitation is expected to stem mainly from electron capture into excited states and from collisions with residual gas molecules just after exit from the ion trap. The cross section for electron capture is quite large and in most charge changing collisions with Na the impact parameter must therefore be so large that there is very little excitation by the recoil of carbon atoms.[34]

With this model we obtain

$$g(\varepsilon, T_{\text{trap}}) \propto \int_0^{\varepsilon} \rho(E) e^{-E/kBT_{\text{trap}}} e^{-\alpha(\varepsilon - E)} dE \propto \exp(-\alpha(\varepsilon - E_0)) \left[1 + \text{erf}\left(\frac{\varepsilon - E_0 - \alpha\sigma^2}{\sqrt{2}\sigma} \right) \right], \tag{3}$$

where E_0 corresponds to the peak of the thermal energy distribution at the ion trap temperature T_{trap}. Here $\rho(E)$ is the vibrational density of states, k_B is Boltzmann's constant, and the parameter in the distribution of excitation energies is chosen to be $\alpha = 1$ eV^{-1}. A Gaussian approximation to the canonical energy distribution in the integral has been used to obtain the last expression, with the standard deviation $\sigma = \sqrt{k_B C T_{\text{trap}}}$.[47] The heat capacity $C(T_{\text{trap}})$ of C_{60} has been evaluated from calculated vibrational frequencies.

The calculations are greatly simplified if this energy distribution of the ensemble of ions is replaced by a distribution in microcanonical temperature, defined by $1/k_B T = d/dE \ln \rho(E)$,

$$g(T, T_{\text{trap}}) \propto \exp(-\alpha'(T - T_{\text{trap}})) \times \left[1 + \text{erf}\left(\frac{T - T_{\text{trap}} - f^2 \alpha' \sigma'^2}{\sqrt{2} f \sigma'} \right) \right], \tag{4}$$

with $\alpha' = \alpha C(T_{\text{trap}})$ and $\sigma' = \sigma / C(T_{\text{trap}})$. A fairly accurate expression for $\rho(E)$ in terms of the partition function (Eq. (24) in Ref. 47) has been used to check the accuracy of the expression in Eq. (4) by numerical evaluation of the integral in Eq. (3). Due to the rapid variation of the heat capacity at low temperatures, a numerical factor f has to be included in the formula, and excellent agreement with the more accurate expression is obtained for the values $f = 1.1$, 1.2, and 1.3 at the three temperatures 355, 300, and 225 K.

The depletion of the temperature distribution is illustrated in Fig. 7 for the lowest trap temperature. It is seen that after 1 ms all ions have an internal temperature well below 400 K, i.e., an internal excitation energy below 1 eV. Hence the experiment only probes this range of excitation energies, and the initial energy distribution need not be as broad as indicated by the curve for 0 ms in Fig. 7. The influence of photon emission and absorption on the distribution after long storage times is discussed in Sec. VIII below.

The rate constant for electron emission is assumed to have two contributions. The first is from tunneling from the two singlet levels ^1A_g and ^1H_g and from the two triplet levels $^3T_{1g}$ and $^3T_{2g}$,

$$k_1(T) = \sum_{i=1}^{4} A_i P_i(T)/Q(T),$$

$$P_i(T) = g_i \exp\left(-\varepsilon_i / k_B \left(T - \frac{\varepsilon_i}{2C(T)} \right) \right), \tag{5}$$

$$Q(T) = \sum_{i=1}^{4} P_i(T).$$

Here ε_i are the four energy levels while g_i and A_i are the corresponding degeneracies and tunneling rates. The effective temperature in the Boltzmann factor is the microcanonical temperature T corresponding to the internal energy ε, with a small finite-heat-bath correction.[47] The parameters used in the fits are given in Table I, and the populations $P_i(T)/Q(T)$ of the four states are illustrated in Fig. 8(a). The two energy separations $\varepsilon_2 - \varepsilon_1$ and $\varepsilon_4 - \varepsilon_3$ are derived from the spectroscopic data, as discussed above. This splitting of the singlet and triplet levels is included for consistency with the spectroscopic data, but equally good fits are obtained without. The average excitation energy of the triplet states is chosen to match the temperature dependence of the data in Fig. 2 and its uncertainty is estimated to be ±10 meV. The

TABLE I. Energies and tunneling rates for the four states included in the modeling.

State	Energy (eV)	Decay rate (s^{-1})
^1A_g	0.200	0.05
^1H_g	0.222	0.70
$^3T_{1g}$	0.305	800
$^3T_{2g}$	0.335	5000

tunneling rates A_i are consistent with the barrier model for $\nu \cong 3 \times 10^{13}$ s^{-1} and $\varepsilon_1 \cong 0.2$ eV.

For relatively high internal energies there must be a rapidly increasing contribution, $k_0(T)$, to the rate constant for electron emission, as evidenced by the power-law decay at short times. This decay is probably dominated by hot-band emission.[48] The product of a room-temperature Boltzmann factor and the WKB barrier-penetration factor has a broad maximum around 0.6 eV, and with the above value of ν, the tunnelling rate is $\sim 10^8$ s^{-1} at this energy. Vibrationally assisted emission is in our model represented by an Arrhenius expression,

$$k_0(T) = A_0 \exp(-\varepsilon_0/k_B T), \tag{6}$$

with $\varepsilon_0 = 0.4$ eV and $A_0 = 7 \times 10^8$ s^{-1}.

This expression is consistent with the observation of rate constants of the order of 10^4 s^{-1} for electron emission from ions with internal temperature around 450 K after absorption of a photon.[44] The two rate constants k_0 and k_1 are in Fig. 8(b) compared with tunneling from the two singlet states alone. This latter contribution is seen to be negligible except for very low temperatures.

The simulated decay rates, normalized to the experiment, are shown together with the channeltron data in Fig. 2. Below room temperature, the emission is dominated by tunneling via thermal population of the triplet states, and their average energy above the ground state and the tunneling rates are determined mainly by the measured spectra in the range of 225–300 K. The calculated decay rates are nearly the same when the two excited levels are replaced by a single level with the average energy and a tunneling rate equal to the geometric average of the two rates. For all trap temperatures, the rate constant k_0 accounts for the yield at the earliest times. It also reduces the cutoff time for high trap temperatures and thereby accounts for the deviation of the corresponding points from the straight line in the Arrhenius plot in Fig. 2.

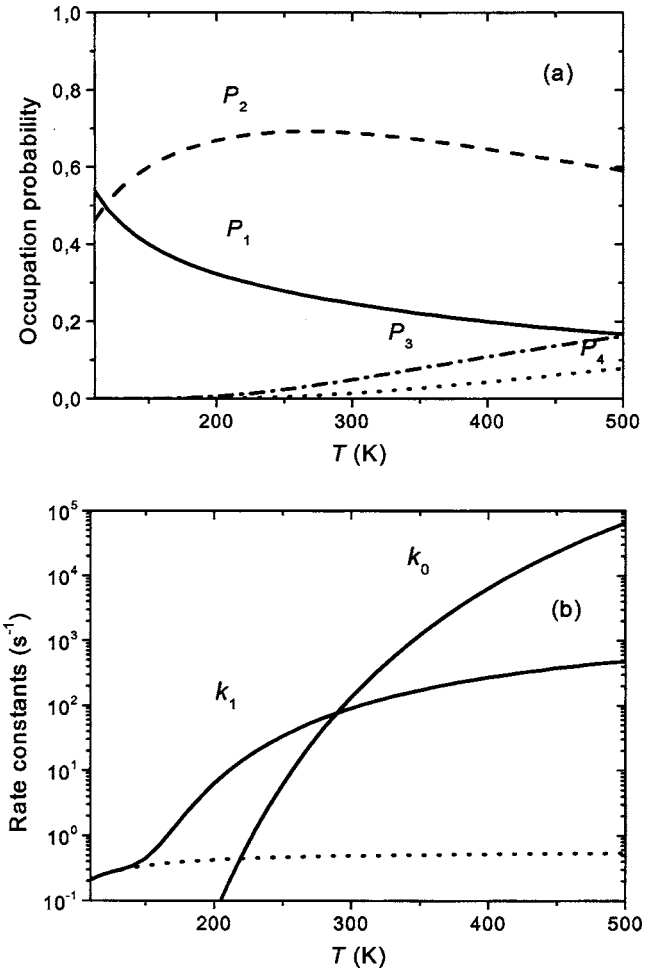

FIG. 8. (a) Populations of the four levels indicated in Fig. 6 as functions of the internal ion temperature (microcanonical). (b) The rate constants for tunneling in Eqs. (5) and (6), and the tunneling rate for electrons confined to the two singlet levels.

VIII. DEPLETION FOR LONG STORAGE TIMES; BLACKBODY RADIATION

The simulations should also account for the measured beam depletion at the two lower trap temperatures in Fig. 3. These measurements follow the decay to later times when only a small fraction of the molecules survive, which have a microcanonical temperature much lower than the trap temperature. The magnitude of the rate constants for tunneling from the singlet states then becomes important for the shape of the decay curves. It turns out that it is not possible to fit simultaneously the two spectra for trap temperatures of 225 and 300 K. With the rate constants given in Table I, the decay curve at room temperature is reproduced reasonably well but, as illustrated in Fig. 3, the measured decay curve for 225 K decreases much more steeply at long times than the calculated one (dotted curve).

An obvious possibility is that the decay is influenced by the absorption and emission of radiation,[49] and this has been included in the full drawn curves in Fig. 3. In neutral C_{60} there are four infrared-active vibrations, each three times degenerate, and as demonstrated by the analysis in Ref. 50, there is quite good agreement between theory and experiment concerning the oscillator strengths. The emission at room temperature corresponds to ~ 0.02 eV/s and the average photon energy is around 0.1 eV. The emission from the fullerene anions should be considerably stronger.[50] For example, the vibrations can "borrow" oscillator strength from the strong $t_{1u} \rightarrow t_{1g}$ transition.[51] We have introduced emission and absorption of 0.1 eV photons with an order of magnitude larger oscillator strength than that for the combined transitions in the neutral molecule, i.e., with an emission and absorption rate of 2 s^{-1} at room temperature. The calculations are analogous to those described in Ref. 52. At low temperatures, the coupling to the blackbody radiation leads to heat-

ing and a more rapid decay, as illustrated by the two energy distributions at 512 ms in Fig. 7. As expected, there is little influence on the decay curve for 300 K, but the agreement with the data for 225 K is much improved (Fig. 3).

According to this analysis, the decay of cold ions is dominated by the absorption of blackbody radiation, leading to the thermal population of the triplet states. This implies that the modeled decay curves are not sensitive to the lifetime of the ground state and the experiment only sets a lower limit of about 1 s for this lifetime. As seen in Table I, the lifetime given by our model is 20 s. This estimate depends somewhat on the choice of the attempt frequency ν in the expression (2) for barrier penetration. Only the decay rates of the triplet states and the relative energies of the four states are determined by measurements, so the position of the lowest-energy level depends on ν, albeit weakly. For example, if ν is reduced by a factor of 5, to $\nu=6\times10^{12}$ s^{-1}, the energies of the triplet states and hence also of the singlet states must be raised by 25 meV, and the tunneling rate from the ground state is then increased by about a factor of 4. Of course there are other uncertainties also; for example, the Franck-Condon factors for electron emission from different states will be different because the Jahn-Teller distortions are not the same.

IX. SUMMARY AND FINAL REMARKS

In summary, we have produced C_{60}^{2-} and C_{70}^{2-} ions in the gas phase from electrospray of the monoanions and subsequent electron capture in collisions with Na atoms. The lifetime of the dianions has been measured in an electrostatic storage ring. While nearly all the C_{70}^{2-} ions are stable on a second time scale, most of the C_{60}^{2-} ions were found to decay on a timescale of milliseconds. The decay is interpreted as mainly thermally assisted tunneling, via excited electronic states or with transfer of energy to the electron from hot vibrational bands. From ESR measurements on dianions in solution a singlet ground state has been deduced, with a thermally populated triplet state ~80 meV above.[8,32] From the similarity of near-infrared absorption in solution and in the gas phase,[44] we conclude that the ground state must be singlet also in the gas phase.

In the modeling we use detailed information on the Jahn-Teller split levels from theory and from gas-phase spectroscopy. The singlet level is split into ^1A_g and ^1H_g, with separation of 22 meV, and the triplet level is split into $^3T_{1g}$ and $^3T_{2g}$, with separation of 30 meV. However, these level splittings have little influence on the modeling of the decay. From the dependence of the decay on the initial temperature of the ions, we deduce a separation of about 120 meV between the singlet ground state and the average energy of two close-lying triplet states. This is similar to the singlet-triplet splitting found in ESR measurements on C_{60} dianions in a matrix, and also to calculations and measurements of the spin gap in A_4C_{60} compounds (A=alkali metal).[26,31] From comparison with a tunneling model, we estimate the position ε_1 of the lowest singlet level to be $+200\pm30$ meV and the lifetime of the ground state to be of the order of 20 s, with an uncertainty of about a factor of 10. The uncertainty of ε_1 is estimated from an uncertainty of an order of magnitude on the tunneling frequency factor ν and ±10 meV on the singlet-triplet separation determined by our fits.

There are still some puzzles left. It is difficult to reconcile our results with the early measurements of quite long-lived C_{60} dianions in ion cyclotron resonance (ICR) traps by Limbach *et al.*[12] and by Hettich *et al.*[13] They saw a strong signal from the dianions in measurements lasting seconds, and the relative amount of singly and doubly charged anions was very similar for C_{60} and C_{70}. In contrast, we have found that while most C_{70}^{2-} ions are stable on a time scale of seconds, nearly all C_{60}^{2-} ions decay on a millisecond time scale. The method of ion production used then, laser ablation of C_{60} deposited on a surface, should certainly not produce colder anions than our method based on electrospray. However, the presence of a very strong magnetic field in the ICR traps could be important. For example, thermal transitions between singlet and triplet states might be hindered by the interaction with this field.

ACKNOWLEDGMENTS

This investigation was supported by a grant from the Danish National Research Foundation to the research center Aarhus Centre for Atomic Physics (ACAP). The collaboration was initiated by the European network LEIF, Contract No. HPRI-CT-1999-40012, and has been supported also by the EU Research Training Network, Contract No. HPRN-CT-2000-0002. It is a pleasure to acknowledge Robert N. Compton for discussions.

[1] M. K. Scheller, R. N. Compton, and L. S. Cederbaum, Science **270**, 1160 (1995).
[2] X.-B. Wang and L.-S. Wang, Nature (London) **400**, 245 (1999).
[3] L.-S. Wang, C.-F. Ding, X.-B. Wang, and J. B. Nicholas, Phys. Rev. Lett. **81**, 2667 (1998).
[4] G. Khairallah and J. B. Peel, Chem. Phys. Lett. **296**, 545 (1998).
[5] O. Hampe, M. Neumaier, M. N. Blom, and M. Kappes, Chem. Phys. Lett. **354**, 303 (2002).
[6] A. Herlert, R. Jertz, J. A. Otamendi, A. J. G. Martinez, and L. Schweikhard, Int. J. Mass. Spectrom. **218**, 217 (2002).
[7] J. Hartig, M. N. Blom, O. Hampe, and M. Kappes, Int. J. Mass. Spectrom. **229**, 93 (2003).
[8] C. A. Reed and R. D. Bolskar, Chem. Rev. (Washington, D.C.) **100**, 1075 (2000).
[9] R. L. Martin and J. P. Ritchie, Phys. Rev. B **48**, 4845 (1993).
[10] C. Yannouleas and U. Landman, Chem. Phys. Lett. **217**, 175 (1994).
[11] W. H. Green, Jr., S. M. Gorun, G. Fitzgerald, P. W. Fowler, A. Ceulemans, and B. C. Titeca, J. Phys. Chem. **100**, 14892 (1996).
[12] P. A. Limbach, L. Schweikhard, K. A. Cowen, M. T. McDermott, A. G. Marshall, and J. V. Coe, J. Am. Chem. Soc. **113**, 6795 (1991).
[13] R. L. Hettich, R. N. Compton, and R. H. Ritchie, Phys. Rev. Lett. **67**, 1242 (1991).
[14] M. C. M. O'Brien, Phys. Rev. B **53**, 3775 (1996).
[15] F. Negri, G. Orlandi, and F. Zerbetto, J. Am. Chem. Soc. **114**, 2909 (1992).
[16] A. V. Nikolaev and K. H. Michel, J. Chem. Phys. **117**, 4761 (2002).
[17] M. Lannoo, G. A. Baraff, M. Schlüter, and D. Tomanek, Phys. Rev. B **44**, 12106 (1991).
[18] M. Schlüter, M. Lannoo, M. Needels, G. A. Baraff, and D. Tomanek, Phys. Rev. Lett. **68**, 526 (1992).
[19] A. Auerbach, N. Manini, and E. Tosatti, Phys. Rev. B **49**, 12998 (1994).
[20] S. Sookhun, J. L. Dunn, and C. A. Bates, Phys. Rev. B **68**, 235403 (2003).
[21] C. C. Chancey and M. C. M. O'Brien, *The Jahn-Teller Effect in C_{60} and other Icosahedral Complexes* (Princeton University Press, Princeton, NJ, 1997).

[22] O. Gunnarsson, H. Handschuh, P. S. Bechthold, B. Kessler, G. Ganteför, and W. Eberhardt, Phys. Rev. Lett. **74**, 1875 (1995).
[23] N. Breda, R. A. Broglia, G. Colò, H. E. Roman, F. Alasia, G. Onida, V. Ponomarev, and E. Vigezzi, Chem. Phys. Lett. **286**, 350 (1998).
[24] S. E. Erwin and W. E. Pickett, Phys. Rev. B **46**, 14257 (1992); , Science **254**, 842 (1992); W. E. Pickett, D. A. Papaconstantopoulos, M. A. Pederson, and S. C. Erwin, J. Supercond. **7**, 651 (1994).
[25] W. E. Pickett, in *Solid State Physics: Advances in Research and Applications*, edited by H. Ehrenreich and F. Spaepen (Academic, New York, 1994), Vol. 48, p. 225.
[26] J. E. Hahn, O. Gunnarsson, and V. H. Crespi, Phys. Rev. Lett. **90**, 167006 (2003); O. Rösch, J. E. Hahn, O. Gunnarsson, and V. H. Crespi, Phys. Status Solidi B **242**, 118 (2005).
[27] R. Friedberg, T. D. Lee, and H. C. Ren, Phys. Rev. B **46**, 14150 (1992).
[28] T. D. Lee, Int. J. Mod. Phys. A **16**, 3785 (2001).
[29] S. Chakravarty and S. A. Kivelson, Phys. Rev. B **64**, 064511 (2001).
[30] M. Capone, M. Fabrizio, C. Castellani, and E. Tosatti, Science **296**, 2364 (2002).
[31] M. Capone, M. Fabrizio, P. Giannozzi, and E. Tosatti, Phys. Rev. B **62**, 7619 (2000).
[32] P. R. Trulove, R. T. Carlin, G. R. Eaton, and S. S. Eaton, J. Am. Chem. Soc. **117**, 6265 (1995).
[33] S. Tomita, J. U. Andersen, E. Bonderup, P. Hvelplund, B. Liu, S. Brøndsted Nielsen, U. V. Pedersen, J. Rangama, K. Hansen, and O. Echt, Phys. Rev. Lett. **94**, 053002 (2005).
[34] B. Liu, P. Hvelplund, S. Brøndsted Nielsen, and S. Tomita, Phys. Rev. Lett. **92**, 168301 (2004).
[35] S. P. Møller, Nucl. Instrum. Methods Phys. Res. A **394**, 281 (1994).
[36] J. U. Andersen, J. S. Forster, P. Hvelplund, T. J. D. Jørgensen, S. P. Møller, S. Brøndsted Nielsen, U. V. Pedersen, S. Tomita, and H. Wahlgreen, Rev. Sci. Instrum. **73**, 1284 (2002).
[37] J. U. Andersen, P. Hvelplund, S. Brøndsted Nielsen, U. V. Pedersen, and S. Tomita, Phys. Rev. A **65**, 053202 (2002).
[38] J. U. Andersen, H. Cederquist, J. S. Forster *et al.*, Phys. Chem. Chem. Phys. **6**, 2676 (2004).
[39] J. U. Andersen, H. Cederquist, J. S. Forster *et al.*, Eur. Phys. J. D **25**, 139 (2003).
[40] K. Hansen, J. U. Andersen, P. Hvelplund, S. P. Møller, U. V. Pedersen, and V. V. Petrunin, Phys. Rev. Lett. **87**, 123401 (2001).
[41] N. G. Gotts, G. von Helden, and M. T. Bowers, Int. J. Mass Spectrom. Ion Process. **149**, 217 (1995).
[42] G. A. Heath, J. E. McGrady, and R. L. Martin, J. Chem. Soc., Chem. Commun. **17**, 1272 (1992).
[43] M. Baumgarten, A. Gügel, and L. Gherghel, Adv. Mater. (Weinheim, Ger.) **5**, 458 (1993).
[44] S. Tomita, J. U. Andersen, E. Bonderup, B. Concina, O. Echt, J. S. Forster, K. Hansen, P. Hvelplund, B. Liu, S. Brøndsted Nielsen, and J. Rangama (unpublished).
[45] M. R. Pederson and A. A. Quong, Phys. Rev. B **46**, 13584 (1992).
[46] O. T. Ehlers, F. Furche, J. M. Weber, and M. M. Kappes, J. Chem. Phys. **122**, 094321 (2005).
[47] J. U. Andersen, E. Bonderup, and K. Hansen, J. Chem. Phys. **114**, 6518 (2001).
[48] X.-B. Wang, C.-F. Ding, and L.-S. Wang, Chem. Phys. Lett. **307**, 391 (1999).
[49] M. N. Blom, O. Hampe, S. Gib, P. Weis, and M. M. Kappes, J. Chem. Phys. **115**, 3690 (2001).
[50] J. U. Andersen and E. Bonderup, Eur. Phys. J. D **11**, 413 (2000).
[51] M. J. Rice and H.-Y. Choi, Phys. Rev. B **45**, 10173 (1992).
[52] J. U. Andersen, C. Gottrup, K. Hansen, P. Hvelplund, and M. O. Larsson, Eur. Phys. J. D **17**, 189 (2001).